Journal of Peptide Science, Vol. 3, 15–30 (1997)

Synthesis, Characterization and Conformational Analysis of gp120-derived Synthetic Peptides That Specifically Enhance HIV-1 Infectivity

MONICA DETTIN[1], ROSSELLA RONCON[1], MARIO SIMONETTI[1], SILVIA TORMENE[1], LUCIA FALCIGNO[2], LIVIO PAOLILLO[2], and CARLO DI BELLO,

[1]Institute of Industrial Chemistry, University of Padua, Italy
[2]Department of Chemistry, University of Naples, Italy

Received 26 February 1996
Accepted 18 April 1996

A series of peptides patterned on the principal neutralizing domain of the HIV-1 envelope glycoprotein gp120 have been synthesized by solid-phase techniques. Interestingly, *in vitro* experiments have shown that some of these peptides specifically interact with CD4 and, in particular, that the peptide corresponding to the sequence 307–330 of the HIV-1 MN isolate was able to enhance infection in a dose-specific and not a strain-restricted way. To bypass problems observed in preliminary runs, several peptides were synthesized by both Fmoc and Boc chemistry. Comparison of the two strategies has allowed the set up of convenient protocols for the preparation of the target peptides in good yield, and with the high-purity grade needed for biological and physicochemical studies. Since the biological effects were present in the carboxyl-free C-terminal linear peptide but not in the amidated C-terminal analogue, preliminary conformational studies by circular dichroism and nuclear magnetic resonance techniques were also performed in an attempt to correlate these effects with possible contributions of structured conformations as predicted by theoretical calculations. The possibility of a β-turn structure for the crucial Gly-Pro-Gly-Arg sequence has been confirmed by 2D NMR experiments. Ongoing studies suggest the exploitation of the activating properties of the MN-derived peptides to design a more sensitive and innovative serological test based on the virus itself and not on anti-HIV antibodies, as is the case for the large majority of tests currently in use.

Keywords: gp120/CD4 interactions; HIV-1 PND; conformation by CD and NMR; solid-phase peptide synthesis

INTRODUCTION

Specific interaction between CD4, the principal receptor on T-cells, and gp120, the external envelope glycoprotein of HIV, triggers virion infection [1]. The protein regions involved in target cell recognition have been defined in some detail [2–10]. In particular, the amino acid residues implicated in CD4 binding have been mapped to the 410–429 region of gp120 [2]. Other gp120 regions seem to act as conformation-inducing determinants, or to contribute to binding [11, 12]. Another gp120 region, distinct from the CD4 binding site, is known as the principal neutralizing domain (PND) of HIV-1, and is required for the production of syncytia [13]. The PND is represented by a disulphide-bridged loop (V3) of the variable region of gp120 that spans residues 303–338, and has been used extensively as an immunogen to elicit neutralizing antibodies [13].

Abbreviations: Abbreviations used for amino acids follow the recommendations of the IUPAC–IUB Commission of Biochemical Nomenclature, *Eur. J. Biochem 138*, 9–37 (1984). BOP, benzotriazol-1-yl-oxy-tris(dimethylamino)phosphonium hexafluorophosphate; 2-Br-Z, 2-bromobenzyloxycarbonyl; CD, circular dichroism; 2-Cl-Z,2-chlorobenzyloxycarbonyl; CE, capillary electrophoresis; DCC, *N*,*N*′-dicyclohexylcarbodiimide; DCM, dichloromethane; DEA, diethylamine; DIEA, diisopropylethylamine; DQFCOSY, double quantum filtered correlated spectroscopy; FAB, fast atom bombardment; FT-IR, Fourier transform infrared; HIV, human immunodeficiency virus; HoHaHa, homonuclear Hartmann–Hahn; HPLC, high performance liquid chromatography; mBHA, 4-methylbenzhydrylamine; NMP, N-methylpyrrolidone; NMR, nuclear magneti resonance; NOESY, nuclear Overhauser enhancement spectroscopy; PAM, phenylacetamidomethyl; Pmc, 2,2,5,7,8-pentamethyl-chroman-6-sulfonyl; PND, principal neutralizing determinant; RP, reversed-phase; SDS, sodium dodecylsulfate; Bu^t, *tert*-butyl; TFE, 2,2,2-trifluoroethanol; TMS, tetramethylsilane; *Trt*, *trityl*.

Address for correspondence: Prof. Carlo Di Bello, Institute of Industrial Chemistry, University of Padova, Via Marzolo 9, 35131 Padova, Italy. Tel. (39-49) 8275547; fax (39-49) 8275550.

CCC 1075-2617/97/010015-16

Owing to its relevance to viral infectivity, therapeutic strategies aimed at blocking CD4 recognition by gp120 have been proposed [14]. To this end, soluble recombinant CD4 or monoclonal antibodies that bind the PND and neutralize the virus have been successfully employed *in vitro* [14–19].

This paper reports the synthesis, purification and characterization of linear peptides patterned on the PND of different HIV-1 isolates (Table 1); some of these peptides were shown to interact with a CD4 site adjacent to, but distinct from, the gp120 binding site. Most interestingly, this specific binding, which mimics the interaction of the viral protein with its cellular target, was shown to enhance syncytia formation and virus infectivity in a dose-specific and not a strain-restricted manner [20, 21]. Since conformational motifs may play an important role in the recognition mechanism and may help in understanding the details of virus pathology at the molecular level, conformational studies, aimed at rationalizing these important biological effects, were also undertaken. Preliminary circular dichroism and nuclear magnetic resonance experiments on these peptides confirm the possible structure of the Gly-Pro-Gly-Arg sequence in a β-turn that could be involved in the recognition process.

MATERIALS AND METHODS

Materials

Boc-protected amino acids and PAM and mBHA resins were obtained from Novabiochem (Langelfingen, Switzerland) and from Bachem California (Torrance, CA, USA), respectively. The chemicals used for Boc peptide synthesis, including TFA, 1 M HOBt/NMP, 1 M DCC/NMP and acetic anhydride were obtained from Applied Biosystems (Forster City, CA, USA); DIEA, methanol and DCM from Janssen (Geel, Belgium); DMSO from Aldrich (Milan, Italy) and NMP from Fluka (Buchs, Switzerland). Fmoc-Gly-*p*-alkoxybenzyl alcohol resin was obtained from Bachem (Bubendorf, Switzerland). Fmoc-amino acids and chemicals used for peptide chemistry were obtained from Applied Biosystems.

Methods

Peptide Synthesis. Peptides patterned on the PND of different HIV-1 isolates were synthesized by solid-phase methods, using a fully automated peptide synthesizer (Applied Biosystems Model 431 A) (Tables 1 and 2).

Synthesis via Boc chemistry. To synthesize amide-terminal peptides, mBHA resin was used as starting solid support, whereas Boc-Gly-PAM resin was used to obtain acid-terminal peptides. The following side-chain protections were employed: Ser and Thr, Bzl; Arg, Tos; Lys, 2-Cl-Z; Tyr, 2-Br-Z; His, Boc. The N_α-Boc protection was removed from all amino acids by a 3 min wash with 25% TFA, followed by a 16 min reaction with 50% TFA in DCM. The coupling media were NMP for the initial 30 min and NMP/DMSO/DIEA for the last 6 min. The incorporation of each residue was followed by a capping cycle, using acetic anhydride (10% acetic anhydride, 5% DIEA in NMP). After the completion of each coupling step, resin samples were collected and a quantitative ninhydrin test was performed to determine the extent of coupling. In the case of DB1 synthesis, coupling yields were $>96\%$, with the exception of Arg^{15} which gave 85.7%. In the case of DB2-NH_2 synthesis, all couplings had a $>98\%$ yield, with the exception of the last step which gave 95%. For DB3, coupling efficiencies were between 97 and 99%, with a reduction to 90% for His^8. In the case of DB3-NH_2

Table 1 Sequence and Derivation of Synthetic Peptides

Name	HIV-1 isolate	Sequence
DB1	IIIB	H-N^1NTRKSIRIQRGPGRAFVTIGKIG^{24}-OH
DB2	RF	H-N^1NTRKSITKGPGRVIYATGQIIG^{23}-OH
DB2-NH_2	RF	H-N^1NTRKSITKGPGRVIYATGQIIG^{23}-NH_2
DB2-Arg^9	RF	H-N^1NTRKSITRGPGRVIYATGQIIG^{23}-OH
DB3	MN	H-Y^1NKRKRIHIGPGRAFYTTKNIIG^{23}-OH
DB3-NH_2	MN	H-Y^1NKRKRIHIGPGRAFYTTKNIIG^{23}-NH_2
DB13		H-Y^1NKRKRIHIQRGPGRAFVTIGKIG^{24}-NH_2

Table 2 Condition of Synthesis

Synthesis	DB1	DB1	DB2	DB2-NH_2	DB2-Arg^9	DB3	DB3	DB3-NH_2	DB13
Strategy	Boc	Fmoc	Fmoc	Boc	Boc	Boc	Fmoc	Boc	Boc
Scale (mmol)	0.50	0.25	0.25	0.50	0.50	0.50	0.25	0.50	0.50
Aa excess	4-fold	4-fold	4-fold	4-fold	4-fold	4-fold	4-fold	4-fold	4-fold
Preactivation	HOBt/DCC	HOBt/DCC	HOBt/DCC	HOBt/DCC	HOBt/DCC	HOBt/DCC	HOBt/DCC	HOBt/DCC	HOBt/DCC
Double couplings	Asn^1-Pro^{13}	Arg^{11}-Gly^{24}	Lys^9-Gly^{23}	All steps	Asn^1-Ile^9	Gly^{12}-Gly^{23}	Gly^{10}, Gly^{12}-Gly^{23}	All steps	All steps
Cleavage	HF/Anisole/ DMS (−5°÷0°C; 60 min)	TFA/H_2O/ Thioanisole/ Ethandithiol/-Phenol (180 min)	TFA/H_2O/ Thioanisole/ Ethandithiol (180 min)	HF/Anisole/ DMS (−5°÷0°C; 60 min)	HF/Anisole/ DMS (−5÷0°C; 60 min)	HF/Anisole/ DMS (−5°÷0°C; 60 min)	TFA/H_2O/ Thioanisole/ Ethandithiol/-Phenol (180 min)	HF/Anisole/ DMS (−5°÷0°C; 60 min)	HF/Anisole/ DMS (−5°÷0°C; 60 min)

synthesis, Ile^7 was the only step with a coupling efficiency lower than 90%, and gave a value of 84%. For DB13, all couplings were $>99\%$. After completion of the synthesis, the peptides were deprotected and cleaved from the resin (Table 2). HF was evaporated with N_2, the residue extracted with cold ethyl ether, and finally with 30% acetic acid solution; the aqueous layer was then lyophilized.

Synthesis via Fmoc chemistry. Peptides DB1, DB2 and DB3 were synthesized by standard Fmoc chemistry, using Fmoc-Gly-*p*-alkoxybenzyl alcohol resin. The side-chain protections employed were: Ser, Thr and Tyr, Bu^t; Lys, Boc; Asn, Gln and His, Trt; Arg, Pmc. Only in case of DB1 was the last Asn residue introduced without side-chain protection. Fmoc removal was accomplished by two washings with 20% piperidine in NMP for 18 min. The coupling medium was NMP with a reaction time of 71 min. After each step, a resin sample was submitted to a quantitative ninhydrin test to determine the extent of coupling. For DB1, coupling efficiency was over 96%, with a reduction to 93% for Thr^{22}, 90% for Asn^{23} and 85% for Asn^{24}. For DB2, all couplings yielded values around 99%, with the exception of the last residue which gave 89%. For DB3, coupling efficiency was between 98% and 99%. After cleavage (Table 2) the resin was filtered, the reaction mixture concentrated, and the peptide precipitated with ethyl ether.

Purification of Peptides Obtained via Boc Chemistry. Crude DB1 was purified by preparative ion-exchange HPLC using a Waters (Milford, MA, USA) SP-5PW column (8×75 mm) under the following conditions: eluent A, 20 mM sodium acetate buffer pH 5; eluent B, 1 M NaCl and 20 mM sodium acetate buffer pH 5; gradient, 0–100% B over 60 min; flow rate, 2.6 ml/min; detected at 254 nm. Fractions containing the target peptide were collected, desalted and further purified by RP-HPLC. Preparative separations were carried out using a Delta Pak C_{18} column (7.8×300 mm; 100 Å, 15 μm) and the following conditions: eluent A, 0.05% TFA in H_2O; eluent B, 0.05% TFA in CH_3CN; gradient, 18–28% B over 30 min; flow rate, 4 ml/min; detected at 214 nm.

Fractions were examined by analytical RP-HPLC and those corresponding to the major peak were collected. The product thus obtained showed a single peak by HPLC that after integration gave a 98.4% purity grade. Purified peptide weighing 45.5 mg was obtained with a global yield of 5% (weight of purified peptide over mg of crude). The electropherogram gave a corrected area of 89.2% under the following conditions: capillary, 72 cm; buffer, 2.5 mM sodium citrate pH 2.5; voltage, 30 kV; temperature, 30°C; injection, by vacuum; detector, 214 nm.

Crude DB2-Arg^9 solution was eluted on an SP-5PW column with the linear gradient described above. After RP-HPLC analysis, peptide-containing fractions were collected and desalted on a Delta Pak C_{18} column using a gradient 15–30% of eluent B (0.05% TFA/CH_3 CN) on eluent A (0.05% TFA/H_2O) over 30 min at a flow rate of 4 ml/min. Finally, the fractions containing the target peptide were chromatographed on a Vydac C_{18} column and gave a single peak with a purity grade of 98.9% (2% yield). Integration of the electropherogram pattern gave a corrected area of 89.3%. The conditions of the analysis were as follows: capillary, 72 cm; buffer, 2.5 mM sodium citrate pH 2.5; voltage, 20 kV; temperature, 30°C; injection, by vacuum; detector, 214 nm.

Purification of crude DB3 started with ion-exchange chromatography on a sulphopropyl column, as described above. After analytical RP-HPLC the fractions corresponding to the major peak were collected and eluted on a Delta Pak C_{18} column using a gradient 15–30% of eluent B (0.05% TFA/CH_3CN) on eluent A (0.05% TFA/H_2O) at a flow rate of 4 ml/min. The purified peptide was loaded on a Vydac C_{18} column. Two mobile phases systems were used: (i) eluent A, 0.05% TFA/H_2O; eluent B, 0.05% TFA/CH_3CN; gradient, 12–27% of B over 30 min; flow rate, 1.5 ml/min; (ii) eluent A, 0.05% TFA, 1.2 g/l tetrabutylammonium hydrogen sulphate in H_2O; eluent B, 0.05% TFA in CH_3CN; gradient, 12–27% of B over 30 min; flow rate, 1.5 ml/min. Both chromatograms confirmed a purity grade of 99%, whereas CE gave a corrected area of 91%. The CE conditions used were the same described for DB2-Arg^9 and the final yield was 2%.

Crude DB13 was loaded on a Protein Pak Glas SP-5PW column and eluted with a gradient 40–60% of 20 mM sodium acetate, 1 M sodium chloride buffer at pH 5.0 on 20 mM sodium acetate buffer (pH 5.0) over 60 min at a flow rate of 2.6 ml/min. After analytical chromatography, the fractions corresponding to the major peak were desalted on a Delta Pak C_{18} using the following conditions: eluent A, 0.05% TFA in H_2O; eluent B, 0.05% TFA in CH_3N; gradient, 20–28% of B over 24 min; detector, 214 and 254 nm. The purified peptide was finally loaded on an analytical column (Vydac C_{18}). A single peak

was obtained at 6.5 min under the following conditions: eluent A, 0.05% TFA in H_2O; eluent B, 0.05% TFA in CH_3CN; gradient, 18–26% of eluent B over 16 min; detector, 214 nm. The yield was 8.7%. HPLC analysis gave a purity grade of 99.5%. CE analysis gave a corrected area of 93.5% under the following conditions: capillary, 72 cm; buffer, 2.5 mM sodium citrate pH 2.5; voltage, 30 kV; temperature, 30°C; injection, by vacuum; detector, 214 nm.

Crude DB2-NH_2 was loaded on a Sephadex G-25SF column (2.7 × 24.3 cm, Pharmacia, Uppsala, Sweden), and eluted with 10% acetic acid. The fractions corresponding to the major peak were lyophilized and chromatographed on a Waters Accell™ CM column (10 × 195 cm) under the following conditions: eluent A, 20 mM sodium acetate, pH 5.0; eluent B, 20 mM sodium acetate and 0.5 M NaCl, pH 5.0; gradient, 0–50% B over 90 min; detector, 214 nm.

Desalting and further purification of the product were achieved by RP-HPLC on a Delta Pak C_{18} column, under the following conditions: eluent A, 0.1 M ammonium acetate and 45 mg/l tetrabutylammonium hydrogen sulphate, pH 5.4; eluent B, 40% eluent A and 60% CH_3 CN; gradient, 28–38% B over 20 min; flow rate, 4 ml/min; detector, 254 nm. The best fractions were loaded on an analytical RP column which confirmed a 96% purity grade. CE analysis gave a 91.6% under the conditions described for DB13 analysis. The yield was 2.3%; other fractions with a lower purity grade were also obtained.

Following HF treatment, crude DB3-NH_2 was concentrated, desalted on a Sephadex G-25 SF

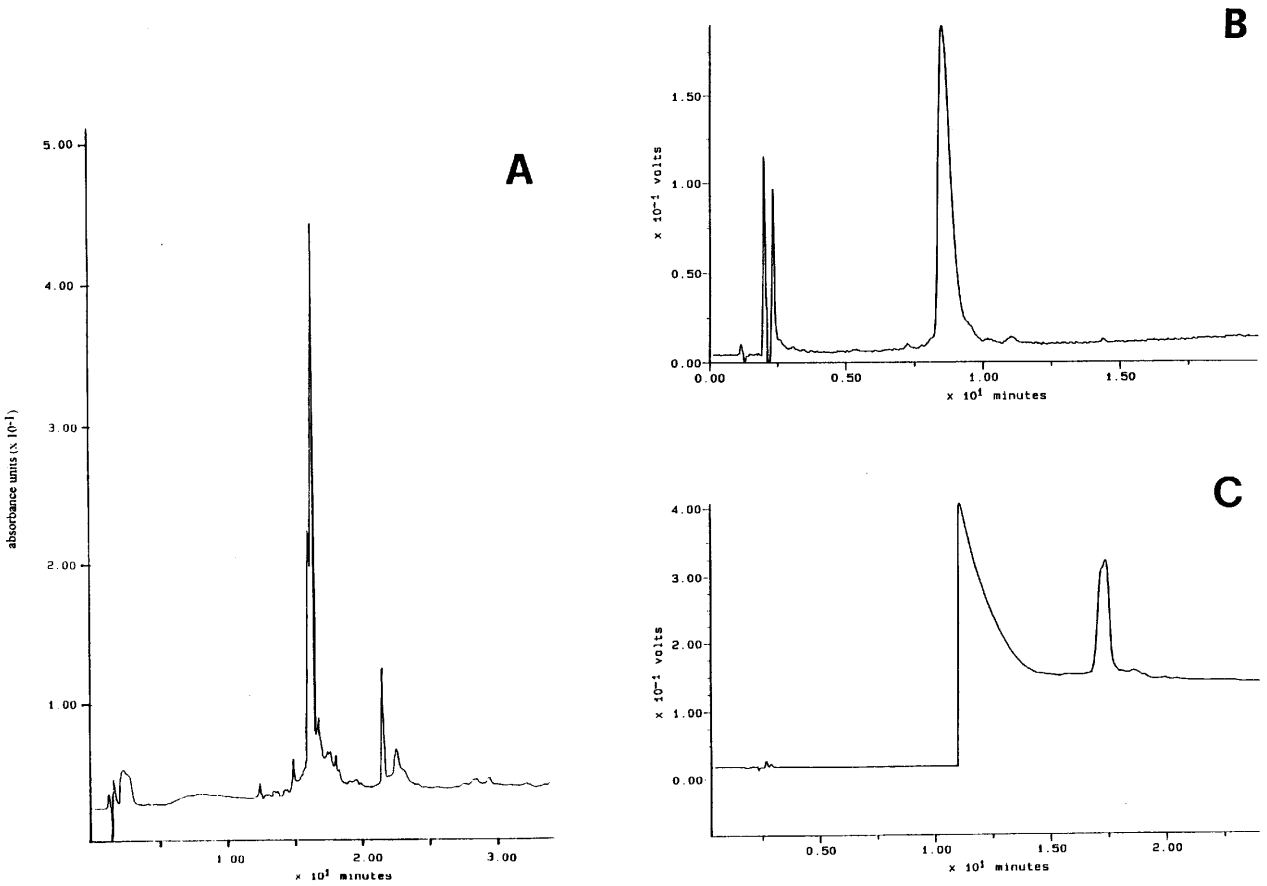

Figure 1 Analytical RP-HPLC of crude DB1 synthesized by Boc chemistry (A) and by Fmoc chemistry (B). Conditions: column, Delta Pak C_{18} (5 μm, 100 Å, 3.9 × 150 mm); eluents, A, 0.05% TFA/H_2O, B, 0.05% TFA/CH_3CN; gradient, 10–50% B over 40 min; flow rate, 1 ml/min; detector, 214 nm. (C) The analytical RP-HPLC of crude DB1 synthesized by Fmoc chemistry in the presence of lipophilic salts. Conditions: column, Vydac C_{18} (5 μm, 4.6 × 250 mm); eluents, A, 0.05% TFA, 1.2 g/l tetrabutylammonium hydrogen sulphate/H_2O, B, 0.05% TFA/CH_3CN; gradient, 3 min at 0% B, 0–10% B in 1 min and 10–20% B in 20 min; flow rate, 1 ml/min; detector, 214 nm.

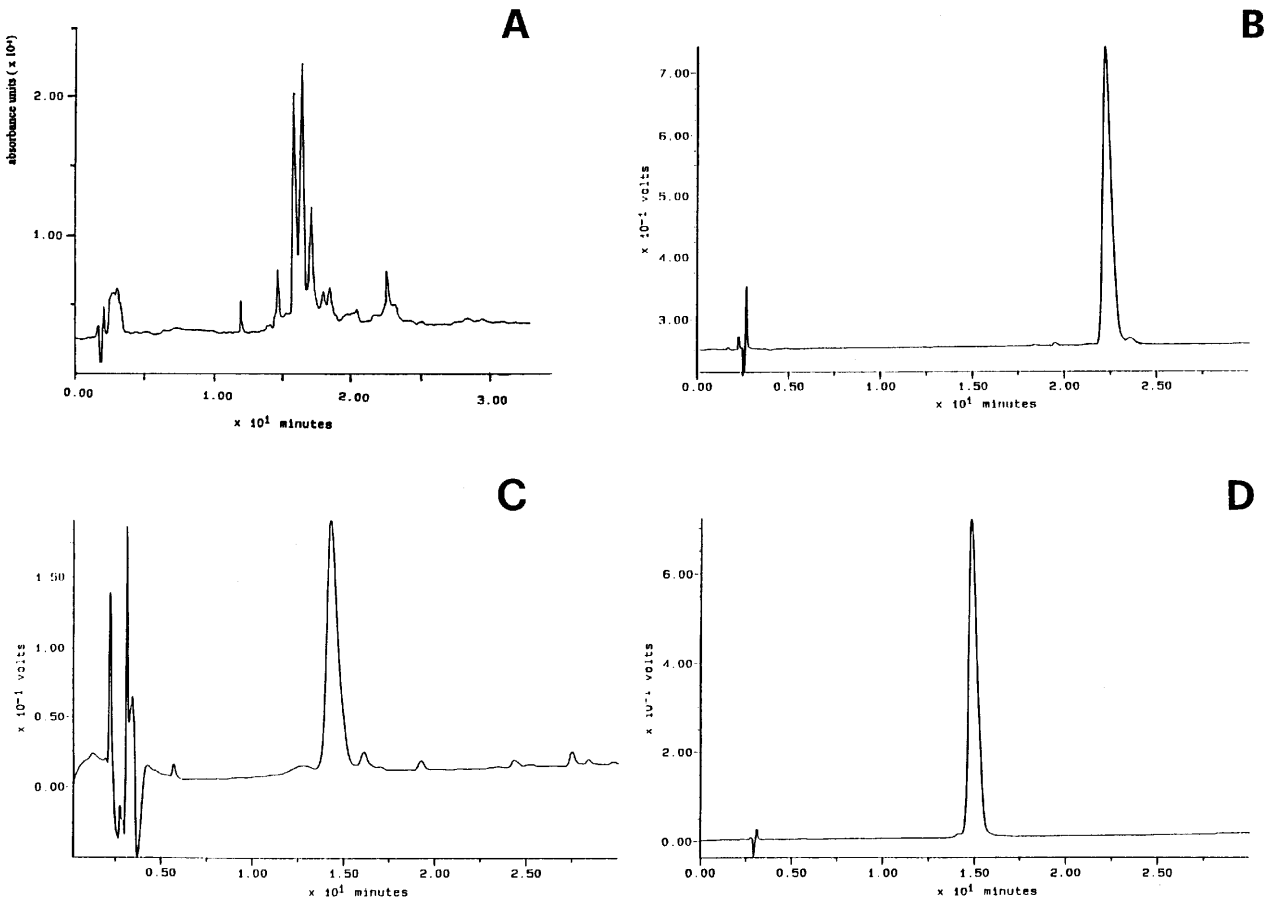

Figure 2 (A): Analytical RP-HPLC of crude DB2-Arg[9]. Conditions: column, Delta Pak C_{18} (5 μm, 100 Å, 3.9 × 150 mm); eluents, A, 0.05% TFA/H_2O, B, 0.05% TFA/CH_3CN; gradient, 10–50% B over 40 min; flow rate, 1 ml/min; chart speed, 0.5 cm/min; sensitivity, 0.5 ABS; detector, 214 nm. (B) Analytical RP-HPLC of purified DB2-Arg[9]. Conditions; column, Vydac C_{18} (5 μm, 4.6 × 250 mm); gradient, 15–30% B in 30 min; flow rate, 1.5 ml/min. (C) Analytical RP-HPLC of crude DB2. Conditions: column, Vydac C_{18}; gradient, 15–30% B in 30 min; flow rate, 1.2 ml/min. (D) Analytical RP-HPLC of purified DB2. Conditions: column, Vydac C_{18}; gradient, 15–30% B in 30 min; flow rate, 1.2 ml/min.

column (2.7 × 24.3 cm, Pharmacia) with 10% acetic acid at a flow rate of 1.25 ml/min, and then purified by preparative ion-exchange HPLC using a Waters Accell™ CM column (1 × 19.5 cm). The column was equilibrated with 20 mM sodium acetate pH 5.0, and eluted with a linear gradient 0–1 M of NaCl over 120 min at a 3 ml/min flow rate. Fractions containing the target peptide were further purified by RP-HPLC using a Delta Pak C_{18} column under the following conditions: eluent A, 0.1 M ammonium acetate, pH 5.4; eluent B, 40% eluent A and 60% CH_3CN; gradient, 28–37% B over 14 min; flow rate, 4 ml/min; detector, 214 nm.

Two eluent systems were used to analyse the purity grade obtained: (i) 25–45% of B (40% A, 60% CH_3CN) on A (0.1 M Na_2HPO_4, 1.2 g/l tetrabutylammonium hydrogen sulphate, pH 5.4) over 22 min at 1.1 ml/min flow rate, and detection at 214 nm; (ii) 20–40% of B (0.1% TFA in CH_3CN) on A (0.1% TFA in H_2O) over 40 min at 1.1 ml/min flow rate and detection at 214 nm. Finally, 103.23 mg of product with a purity grade of 97% were obtained. A CE analysis gave a corrected area value of 84% under the following conditions: capillary, 72 cm; buffer, 2.5 mM sodium citrate pH 2.5; voltage; 20 kV; temperature, 30°C; injection by vacuum; detector, 214 nm.

Purification of Peptides Obtained via Fmoc Chemistry. Crude DB1 synthesized via Fmoc chemistry presented twin peaks with a very similar retention time, as shown in the RP chromatogram in Figure

Table 3 Amino Acid Analyses of Synthetic Peptides After Acid Hydrolysis

AA	DB1^{Boc}	DB1^{Fmoc}	DB2-Arg^{9Boc}	DB2^{Fmoc}	DB2-NH_2	DB3^{Boc}	DB3^{Fmoc}	DB3-NH_2	DB13
Asp	1.8(2)[a]	1.9(2)	1.8(2)	1.8(2)	2.0(2)	2.0(2)	2.0(2)	2.3(2)	0.8(1)
Glu	1.1(1)	1.0(1)	1.3(1)	1.0(1)	1.1(1)				0.9(1)
Ser	0.9(1)	0.9(1)	0.9(1)	0.9(1)	0.9(1)				
Gly	3.9(4)	3.9(4)	4.0(4)	4.1(4)	4.2(4)	3.1(3)	3.0(3)	2.8(3)	3.9(4)
His						0.9(1)	1.0(1)	0.9(1)	0.9(1)
Arg	4.0(4)	3.9(4)	3.1(3)	2.0(2)	2.1(2)	3.1(3)	3.1(3)	3.1(3)	3.9(4)
Thr	2.0(2)	2.0(2)	3.0(3)	3.5(3)	2.9(3)	2.0(2)	2.1(2)	2.1(2)	1.1(1)
Ala	1.0(1)	1.0(1)	1.0(1)	1.0(1)	1.1(1)	1.1(1)	1.0(1)	1.0(1)	0.9(1)
Pro	1.0(1)	1.0(1)	1.0(1)	1.0(1)	1.1(1)	1.1(1)	1.0(1)	1.4(1)	1.0(1)
Tyr			1.0(1)	1.0(1)	1.0(1)	2.0(2)	1.9(2)	2.1(2)	0.9(1)
Val	1.0(1)	1.0(1)	0.8(1)	0.8(1)	0.9(1)				1.1(1)
Ile	4.0(4)	3.9(4)	3.2(4)	3.5(4)	3.4(4)	3.5(4)	3.6(4)	3.2(4)	3.6(4)
Phe	0.9(1)	1.0(1)				1.0(1)	1.0(1)	1.1(1)	1.0(1)
Lys	1.9(2)	2.0(2)	1.4(1)	2.1(2)	2.0(2)	2.9(3)	3.0(3)	2.5(3)	2.8(2)

[a]Theoretical values.

1(c). A better separation of the two peaks was achieved by ion-exchange chromatography using a Waters Protein Pak Glass column (sulphopropyl resin, 10 μm, 8 × 75 mm) under the following conditions: eluent A, 80% 50 mM sodium acetate, 0.1 M NaCl, pH 5.5 and 20% CH_3CN; eluent B, 80% 50 mM sodium acetate, 1 M NaCl, pH 5.5 and 20% CH_3CN; gradient, 40–50% of B over 20 min; flow rate, 2.6 ml/min; detector, 250 nm. After RP analytical chromatography, the fractions containing the target peptide were collected and desalted on a Delta Pak C_{18} column.

The final analytical chromatogram on a Vydac C_{18} column gave a 99.3% of purity grade under these conditions: eluent A, 0.05% TFA in H_2O; eluent B, 0.05% TFA in CH_3CN; flow rate, 1.5 ml/min; gradient, 21–29% of B over 16 min; detector, 214 nm. A corrected area of 91.3% was obtained from the CE pattern. The parameters were the same as those used for the DB3-NH_2 analysis. The yield of purified peptide was 16%.

Crude DB2 was purified by RP chromatography on a semi-preparative Delta Pak C_{18} column under the following conditions: gradient, 20–26% of eluent B (0.05% TFA in CH_3CN) on eluent A (0.05% TFA in H_2O) over 12 min; flow rate, 4 ml/min; detector, 214 and 254 nm. The fractions corresponding to the major peak were collected and lyophilized.

Analytical chromatography on a Vydac C_{18} column with the conditions reported in Figure 2(D) confirmed a purity grade of 99.3%. Pure peptide weighing 260 mg was obtained with a yield of 63%. CE analysis gave a corrected area of 74.0% under the following conditions: capillary, 72 cm; buffer, 2.5 mM sodium citrate pH 2.5; voltage, 30 kV; temperature, 30°C; injection by vacuum; detector, 214 nm. Crude DB3 was chromatographed on a Delta Pak C_{18} column with a mobile phase ranging from 10% of eluent B (0.05% TFA in CH_3CN) on eluent A (0.05% TFA in H_2O) to 30% of B over 40 min. Collection and lyophilization of the fractions corresponding to the major peak gave 319.7 mg of peptide at 100% purity grade with a total yield of 17%. The electropherogram of purified peptide confirmed the HPLC data (100% corrected area). The CE conditions were the same as those used for the DB2 analysis. Edman degradation of all the peptides gave the expected sequences. FAB mass spectrometry confirmed the expected molecular mass for all the peptides. The results of the amino acid analyses are reported in Table 3. The nonquantitative result for Ile is probably due to incomplete hydrolysis of the Ile-Ile sequence; indeed, for DB3, the experimental Ile value approaches the theoretical value when the hydrolysis time is extended to three days.

HPLC Experiments. Preparative and analytical RP-HPLC experiments were performed using a Waters chromatograph equipped with a solvent delivery system model 6000A, a pump model 510, a detector model 441A and an automatic injector Wisp model 712. A Maxima 820 (Waters) chromatography workstation was used to store and integrate the chromatograms. Ion-exchange liquid chromatography was performed on a Waters Advanced Protein Purification Systems model 660, equipped with an adsorbance detector model 440.

Amino Acid Analysis. Peptide hydrolyses were performed at 110°C for 24 h with 6N HCl under vacuum. The amino acids were functionalized with phenylisothiocyanate, and separated using RP-HPLC.

Edman Degradation. Edman degradations were performed on an Applied Biosystems 470 A gas-phase protein sequencer.

Capillary Electrophoresis. Electropherograms of the purified peptides were obtained on an Applied Biosystems analytical capillary electrophoresis system model 270 A.

CD Measurements. CD spectra were performed at room temperature (~25°C) using a Jasco model J-710 automatic recording circular dichrograph equipped with a dedicated data processor. Cylindrical fused quartz cells of 0.05 cm path length were employed. The CD instrument was standardized with D-10-camphorsulphonic acid and epi-androsterone. Spectra are reported in units of mean residue ellipticity (peptide molecular weight/number of amino acids $[-]_R$ (deg cm^2/dmol). Peptide samples were prepared by dissolving weighed quantities in a minimum amount of H_2O to which TFE, phosphate buffer or SDS solution was added up to a final content of 99% (v/v). Peptide concentrations ranged from 4.3 to 6.4 × 10^{-5} M.

NMR Measurements. NMR studies were carried out on a Varian Unity 400 spectrometer. The solutions were prepared by dissolving 4–6 mg of each peptide in 0.7 ml of DMSO-d6 (99.99% isotopic purity, Aldrich). NMR chemical shifts were referred to internal TMS. Proton chemical shift assignments

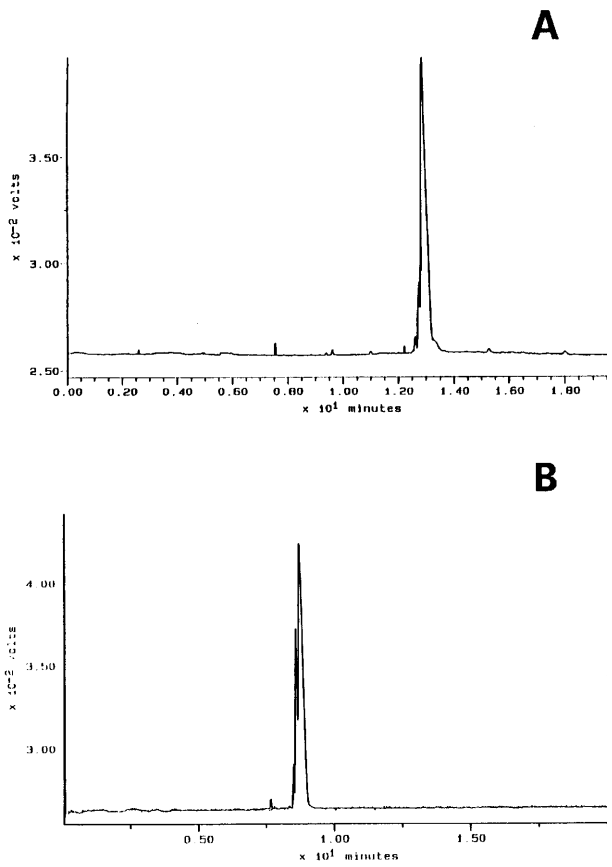

Figure 3 (A) Electropherogram of purified DB2-Arg^9. Conditions: capillary, 72 cm; buffer, 20 mM sodium citrate pH 2.5; voltage, 20 kV; temperature, 30°C; injection by vacuum; run time, 20 min; detector, 214 nm. (B) electropherogram of purified DB2. Conditions: voltage, 30 kV.

were made with the aid of 2D techniques, such as DQFCOSY [22], HoHaHa experiments [23] and NOESY [24].

RESULTS

Peptide Synthesis and Purification

A set of peptides derived from the PND of the gp120 viral glycoprotein (Table 1) was synthesized by solid-phase methods. In order to overcome a few problems encountered during preliminary syntheses and to optimize the synthesis and purification protocols, some of the peptides were synthesized by both Boc and Fmoc strategies. As a general trend, crude peptides obtained by the Boc strategy showed rather complex HPLC patterns, while crude peptides made via Fmoc chemistry seemed more homogeneous, possibly due to a better separation of the scavengers from the deblocking reaction mixture. Typical examples are shown in Figures 1 and 2. Furthermore, the final yield of the purified products obtained via Fmoc chemistry was usually four-fold higher. Specific problems concerning the synthesis and purification of the different peptides by the two methods are discussed below.

In the case of peptide DB1, the simplicity of the HPLC pattern of the crude peptide obtained by the Fmoc chemistry using classical buffers (Figure 1(B) is only apparent; indeed, using eluents enriched with lipophilic salts, twin peaks with very close retention times were evidenced by RP-HPLC (Figure 1(C). Their separation was achieved by ion-exchange chromatography on a sulphopropyl resin, loading fractions up to 20 mg. Amino acid analysis of the two components, after acid hydrolysis, gave the same result; moreover, Edman degradation showed that the sequence of the two peptides was identical. However, FAB mass spectrometry showed that the first peptide eluted in ion-exchange chromatography had a dehydrated Asn residue; the identity of this side product was confirmed chemically by quantitative reconversion to Asn by treatment with H_2O_2/OH^-. The amount of nitrile side product observed was surprisingly high ($\sim$47%) since, in the presence of HOBt, dehydration of Asn to the corresponding nitrile is usually limited to 4% [25].

In the DB2 synthesis, protection of the two Asn residues by the Trt group completely prevented dehydration, and the degree of DB2 purity reached by Fmoc chemistry was similar to that of its analogue DB2-Arg^9 obtained by Boc chemistry (Figure 2(B) and (D). However, CE analysis evidenced a higher complexity in the products obtained by Fmoc chemistry (Figure 3(B)).

The Fmoc strategy presented clear advantages over the Boc method, especially for DB3 synthesis, where a final product in high yield and without impurities was obtained. The well-known observation of considerable, irreversible losses of material during ion-exchange chromatography was also confirmed in the case of the present peptides.

Conformational Studies

CD and 2D NMR conformational studies were carried out in an attempt to study the secondary structure of the peptides, and, hopefully, to correlate their conformation to the biological activity.

The CD spectra of DB1, DB3 and DB3-NH_2 in 10 mM phosphate buffer (pH 6) showed an intense negative band at 197–199 nm (Figure 4(A)). Under

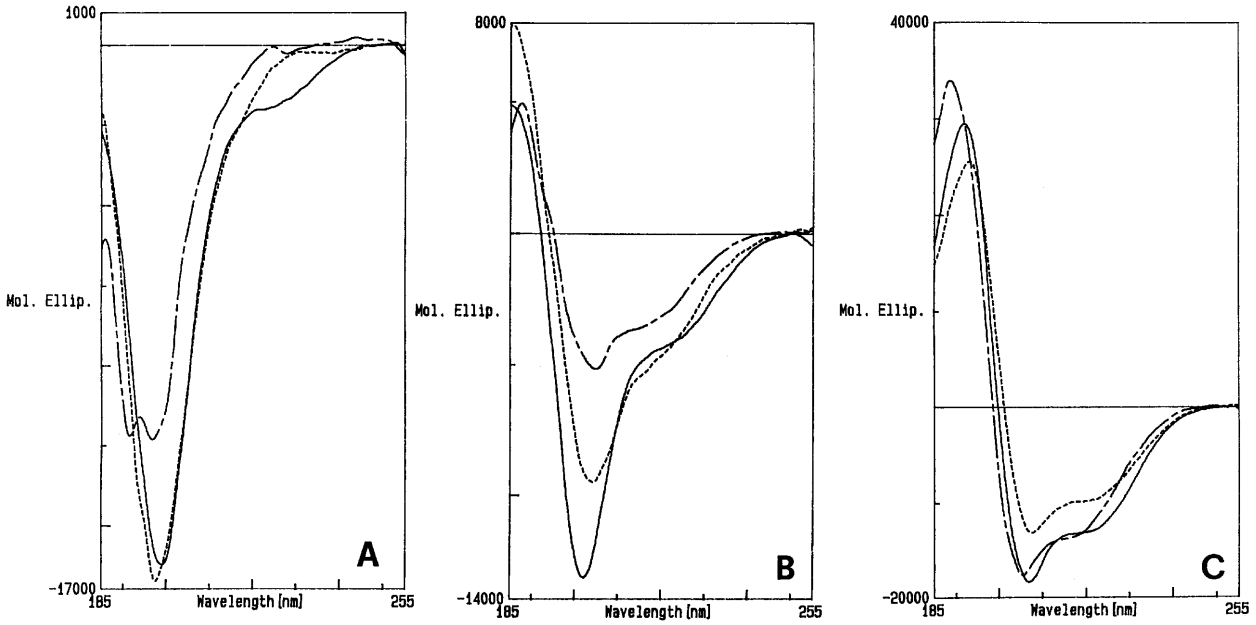

Figure 4 CD spectra of DB1 (-), DB3 (- - -) and DB3-NH_2 (– – –), in 10 mM phosphate buffer pH 6 (A), in 14 mM SDS (B) and in TFE (C).

these conditions, none of the peptides displayed ordered structures, as also confirmed by the high percentage of random conformation indicated by the Lincomb Program (Table 4 [26]). The profiles changed in going from an aqueous solution to a membrane-like environment. In 14 mM SDS, the peptide $\pi \rightarrow \pi^*$ transition was red-shifted to 202 nm for DB1, and to 204 nm for DB3 and DB3-NH_2 (Figure 4(B), while a shoulder appeared at 215–220 nm for all peptides. These properties indicate that, even though an unordered conformation is still predominant, a transition to a more ordered structure, probably an antiparallel β-sheet, occurs in this hydrophobic environment. In TFE the profiles were similar for all peptides. Three bands were observed (Figure 4(C): a more intense positive one at $\sim$192 nm, and two negative at $\sim$207 nm and at about 222 nm. The ratios between the intensities of the three bands changed, while the bands for the biologically inactive DB3-NH_2 were all slightly blue-shifted. This result confirms the high capability of TFE to induce α-helical structures even in peptides that present amino acid sequences without a high α-helix propensity; in this particular case, three consecutive α-helix breakers (GPG) are present in the central part of the sequence.

Table 4 Quantification of Secondary Structures from CD Spectrum Data by the Lincomb Method

Peptide	Buffer	α-Helix (%)	β-Turn (%)	β-Sheet (%)	Random (%)
DB1	10 mM phosphate buffer			10	90
DB3	10 mM phosphate buffer			13	87
DB3-NH_2	10 mM phosphate buffer			20	80
DB1	14 mM SDS			23	77
DB3	14 mM SDS	10		20	70
DB3-NH_2	14 mM SDS	7		32	61
DB1	TFE	17	24		59
DB3	TFE	47	4	6	43
DB3-NH_2	TFE	30	15		55

Table 5 Noe connectivities observed in NOESY spectra of DB3 and DB3-NH2. Grey zones indicate resonance overlapping

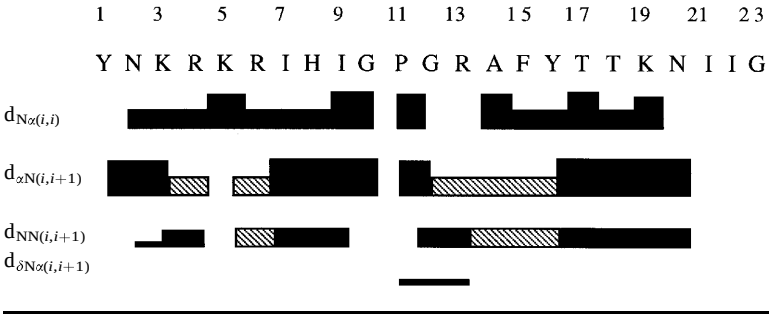

Table 6 Coupling Constants from 2D DQFCOSY of Peptides DB3 and DB3-NH_2 in DMSO at 298 K

AA	$^3J_{NH\alpha CH}$ (Hz)		AA	$^3J_{NH\alpha CH}$ (Hz)	
	DB3-NH_2	DB3		DB3-NH_2	DB3
Tyr^1	6.5		Arg^{13}	8.2	7.7
Asn^2	7.4	7.9	Ala^{14}	8.1	
Lys^3	7.1	7.9	Phe^{15}	8.3	7.9
Arg^4	9.1	7.9	Tyr^{16}	12.5	7.9
Lys^5	8.5	8.5	Thr^{17}	8.4	7.9
Arg^6			Thr^{18}	8.4	8.1
Ile^7	8.4	7.7	Lys^{19}		7.7
His^8	8.6	10.6	Asn^{20}	6.5	7.8
Ile^9		8.1	Ile^{21}	8.4	7.9
Gly^{10}			Ile^{22}	6.5	7.9
Pro^{11}			Gly^{23}		
Gly^{12}					

2D NMR studies in DMSO were conducted on DB1, DB3 and DB3-NH_2. The biologically active DB3 revealed a complete sequence of medium and consecutive $d_{NN(i,i+1)}$ NOEs observed throughout the peptide, except for the two Arg^4-Lys^5 and Lys^5-Arg^6 sequences (Table 5). In particular, the $d_{\alpha N(i,i+1)}$ NOEs were more intense than the $d_{NN(i,i+1)}$ NOEs and were detected for all amino acids except NHLys^5-αArg^4. Resonance overlapping did not permit NOE contacts to be distinguished in the Arg^{13}-Thr^{17} segment. These results indicate a stronger preference for an extended chain or β-sheet conformation with respect to an α-helix conformation. Interestingly, the NOE contacts between NHGly^{12}-NHArg^{13} and αGly^{12}-NHArg^{13} can be associated with the presence of a β-turn structure for the Gly-Pro-gly-Arg sequence, though the αCHPro^{11}-NHArg^{13} NOE contact, which is diagnostic for such a conformation, could not be unambiguously assessed because of spectral overlapping. The DMSO $^3J_{NH\alpha CH}$ values (Table 6) were typical of averaged conformations. Our present data in DMSO, indicating the presence of a β-turn structure in the Gly-Pro-Gly-Arg sequence of DB3, are in line with the observation that the Gly-Pro-Gly tripeptide of a DB3 analogue, bearing a Cys residue as its C-terminal residue, tended to assume a β-turn

Table 7 NOE Connectivities Observed in NOESY Spectrum of Peptide DB1. Non-Integrable NOE Contacts (white) and Resonance Overlapping (Grey) are Indicated

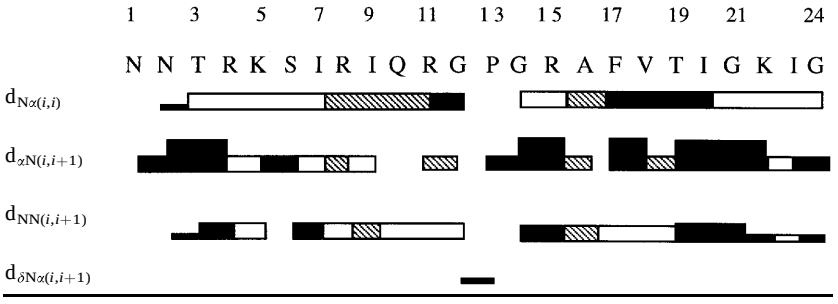

Table 8 Proton Chemical Shift of DB1, DB3 and DB3-NH_2 in DMSO at 298 K

AA	NH	αCH	αα′CH_2	βCH	ββ′CH_2	γγ′CH_2	γCH_3	δδ′CH_2	δCH_3	εε′CH_2	Others
						DB1					
Asn^{1}		4.08			2.68, 2.56						7.70, 7.28 ($CONH_2$)
Asn^{2}	8.72	4.70			2.61, 2.43						7.50, 7.00 ($CONH_2$)
Thr^{3}	7.86	4.10		4.05			1.07				4.96(OH)
Arg^{4}	7.98	4.29			1.71	1.52		3.10			7.62(εNH_2)
Lys^{5}	7.98	4.29			1.70	1.30		1.50		2.75	7.69 (εNH_2)
Ser^{6}	8.01	4.34			3.55						5.02 (γOH)
Ile^{7}	7.79	4.21		1.75		1.10	0.85		0.85		
Arg^{8}	8.09	4.32			1.67	1.50		3.10			7.62 (εNH_2)
Ile^{9}	7.85	4.18				1.10	0.84		0.84		
Gln^{10}	8.08	4.26			1.73	2.10, 1.84					
Arg^{11}	8.01	4.32			1.70	1.50		3.09			7.56 (εNH_2)
Gly^{12}	8.09		3.85, 4.03								
Pro^{13}		4.3			2.02	1.90		3.45, 3.55			
Gly^{14}	8.14		3.68								
Arg^{15}	7.85	4.3			1.60	1.41		3.06			7.56 (εNH_2)
Ala^{16}	8.08	4.26									1.18 (βCH_3)
Phe^{17}	8.04	4.56			3.02, 3.80						
Val^{18}	7.92	4.30		1.98			0.84				
Thr^{19}	7.92	4.30		4.00			1.02				4.93(OH)
Ile^{20}	7.66	4.21		1.72		1.12	0.88		0.88		
Gly^{21}	8.18		3.79, 3.67								
Lys^{22}	7.89	4.32			1.50	1.28		1.63		2.76	7.69 (εNH_2)
Ile^{23}	7.81	4.20		1.72		1.12	0.82		0.82		
Gly^{24}	8.28		3.80, 3.70								16.4 (COOH)
						DB3					
Tyr^{1}	8.08	3.95			3.00, 2.75						6.74 (3H,5H); 7.06 (2H,6H)
Asn^{2}	8.81	4.63			2.61, 2.47						7.59, 7.04 ($CONH_2$)
Lys^{3}	8.23	4.20			1.74	1.34		1.53		2.73	7.70 (εNH_3)
Arg^{4}	8.07	4.28			1.65	1.50		3.09			7.74 (NH)
Lys^{5}	7.89	4.23			1.70	1.32		1.53		2.74	7.83 (NH)
Arg^{6}	8.03	4.22			1.72	1.54		3.09			7.75 (NH)
Ile^{7}	7.80	4.19		1.37		1.04	0.78		0.78		
His^{8}	8.34	4.66			3.03, 2.91						8.92, 7.28 (2H,4H)
Ile^{9}	7.86	4.20		1.68		1.06	0.78		0.82		
Gly^{10}	8.16		4.01, 3.83								
Pro^{11}		4.31			2.03	1.86		3.57, 3.48			
Gly^{12}	8.19		3.70								
Arg^{13}	7.84	4.29			1.61	1.42		3.04			7.54 (NH)
Ala^{14}	8.03	4.24									1.12 (βCH_3)
Phe^{15}	7.94	4.45			2.96, 2.74						7.19 (2H,6H); 7.04 (3H,5H)
Tyr^{16}	8.03	4.58			2.95, 2.72						7.05 (2H,6H); 6.64 (3H,5H)
Thr^{17}	8.06	4.40		4.04			1.06				5.06 (OH)
Thr^{18}	7.70	4.27		4.06			1.08				4.98 (OH)
Lys^{19}	7.94	4.28			1.66	1.32		1.52		2.73	7.70 (εNH_3)
Asn^{20}	8.19	4.57			2.55, 2.37						7.40,6.95 ($CONH_2$)
Ile^{21}	7.72	4.28		1.44		1.08	0.80		0.78		
Ile^{22}	7.77	4.18		1.74		1.06	0.84		0.77		
Gly^{23}	8.34		3.84,3.66								14.2 (COOH)

(*Continued*)

Table 8 "Continued"

AA	NH	αCH	αα′CH_2	βCH	ββ′CH_2	γγ′CH_2	γCH_3	δδ′CH_2	δCH_3	εε′CH_2	Others
					DB3-NH_2						
Tyr^1	8.05	3.96			3.05, 2.77						6.63 (3H, 5H); 7.04 (2H, 6H)
Asn^2	8.81	4.65			2.61, 2.47						7.58, 7.07 ($CONH_2$)
Lys^3	8.27	4.21			1.72	1.34		1.53		2.76	7.74 (εNH_3)
Arg^4	8.10	4.31			1.66	1.50		3.10			7.77 (NH)
Lys^5	7.92	4.21			1.76	1.30		1.52		2.74	7.74 (NH)
Arg^6	8.06	4.22			1.73	1.56		3.10			7.77 (NH)
Ile^7	7.83	4.20		1.68		1.37	1.06		0.78		
His^8	8.34	4.69			3.04, 2.93						8.92, 7.32 (2H,4H)
Ile^9	7.91	4.23		1.75		1.10	0.84		0.84		
Gly^{10}	8.14		4.02, 3.82								
Pro^{11}		4.34			2.02	1.89		3.58, 3.49			
Gly^{12}	8.22		3.68								
Arg^{13}	7.87	4.29			1.61	1.44		3.04			7.59 (NH)
Ala^{14}	8.02	4.22									1.14 (βCH_3)
Phe^{15}	7.98	4.46			2.96, 2.76						7.17 (2H,6H); 7.05 (3H,5H)
Tyr^{16}	8.06	4.59			2.98, 2.75						7.05(2H,6H); 6.71 (3H,5H)
Thr^{17}	8.10	4.41		4.06			1.06				
Thr^{18}	7.73	4.25		4.10			1.06				
Lys^{19}	7.97	4.28			1.66	1.32		1.52		2.74	7.85 (εNH_3)
Asn^{20}	8.23	4.59			2.56, 2.39						7.41, 6.95 ($CONH_2$)
Ile^{21}	7.75	4.28		1.72		1.52	1.32		0.82		
Ile^{22}	7.91	4.08		1.75		1.06	0.82		0.82		
Gly^{23}	8.05		3.68, 3.57								7.27, 7.16 ($CONH_2$)

structure even in H_2O [27]. These conclusions were based on the presence of NOE contacts between $NHGly^{12}$-$NHArg^{13}$, α$CHPro^{11}$-$NHArg^{13}$, δPro^{11}-$NHGly^{12}$ and of an extremely weak α$CHPro^{11}$-$NHGly^{12}$ NOE. The NOEs' pattern, coupling constants and temperature coefficients of the amide protons of our DMSO spectra correspond closely to the spectra obtained in H_2O and the analogy is so close as to include the lack of some NOEs such as that between $NHArg^4$-$NHLys^5$.

The NOESY spectra in DMSO of the less active DB1 showed a sequence of $d_{NN(i,i+1)}$ effects in the Gly^{14}-Gly^{24} region, except for the 17–18 and 22–23 connectivities (Table 7). The intensity ratio between $d_{\alpha N(i,i+1)}$ NOEs and $d_{NN(i,i+1)}$ NOEs confirms the absence of a significant population of α-helix conformers. These data are in line with the lack of long-range contacts, typical of an α-helix structure. In the Gly-Pro-Gly-Arg region, only medium strength NOEs between $NHGly^{14}$-$NHArg^{15}$ and $NHGly^{14}$-αPro^{13} were observed, while the $NHGly^{14}$-δPro^{13} NOE effect, indicative of a type I β turn [28], was absent. The $NHArg^{15}$-αPro^{13} could not be clearly identified since the chemical shifts of α$CHArg^{15}$ and α$CHPro^{13}$ coincide. Strong NOE contacts between Hαα′Gly^{12}-Hδδ′Pro^{13} protons indicated that the Gly^{12}-Pro^{13} linkage adopts a *trans* configuration.

The inability of amide-terminal peptides to interact with immobilized CD4 and to enhance virus infectivity is noteworthy. Interestingly, the ability of peptide DB3 to enhance virus infectivity was lost by substituting the carboxylic function with a C-terminal amide moiety. 2D NMR studies in DMSO, however, did not reveal specific differences between DB3 and DB3-NH_2 (Table 8); as a matter of fact, the only variations observed concerned the Ile^{22} and Gly^{23} residues, as a consequence of the different C-terminal functionality.

DISCUSSION

Synthetic peptides have found widespread application in the field of AIDS, particularly to study the mechanism that permits virus entry into target cells, and to detect immunosilent regions. Peptides have also been employed in diagnostic tests and for the design of potential inhibitors of the viral proteases [29, 30].

The V3 loop of gp120, that contains the PND of HIV-1 viruses, plays a critical role in viral infectivity and tropism. The amino acid sequence of the PND is highly variable, except for a short stretch at the tip of the V3 loop. Several lines of evidence have already indicated that this region may adopt a conserved structure in different HIV-1 isolates.

Competition experiments using epitope-specific mAbs have shown that synthetic peptides corresponding to the PND of different HIV-1 isolates were specifically recognized by a CD4 site adjacent to, but distinct from, the gp120 binding site [21]. More interestingly, these peptides were shown to enhance syncytia formation and virus infectivity in a dose-specific and not a strain-restricted manner [20]. Our hypothesis of a secondary binding role for the V3 loop is in line with the observation that neutralizing antibodies directed to the V3 loop are able to block virus entry even after biding involving the two principal binding regions of gp120 and CD4. Moreover, mutations in the V3 loop generate non-infectious viruses that can still bind to CD4. As the virus activation properties of DB3 are maintained even when peptide DB3 is added to blood samples of seropositive patients, a more sensitive and innovative serological assay based on direct virus detection is now under study [31]. A particular advantage of this new method is that it may be used to determine the presence of HIV in a patient who has not been infected long enough to produce anti-HIV antibodies: there is a 'window' period between the start of the infection and the appearance of specific anti-HIV antibodies that may last up to a year [32].

Since the presence of structural elements could be of crucial importance in order to understand the complex mechanism of recognition and interaction between gp120 and CD4, a conformational study on these synthetic gp120-related peptides, using Chou-Fasman and spectroscopical approaches, was also started [33]. As expected, the CD studies confirmed the high flexibility typical of linear peptides and showed that the rapid equilibrium between different conformations is shifted towards ordered populations on going from an aqueous to a more hydrophobic environment. Interestingly, the presence of a β-turn for the Gly-Pro-Gly-Arg sequence, recently proposed by La Rosa *et al.* [34], using a neural network approach, has been confirmed by our present 2D NMR experiments in DMSO. Moreover, the presence of this structural motif has been described by Chandrasekhar *et al.* by NMR studies in H_2O in a peptide closely related to DB3 [27].

The above conformational results are in good agreement with a theoretical model we have recently proposed for the biologically active conformer of DB3 [33]. In this model, the highly preserved Gly^{10}-Pro-Gly-Arg^{13} sequence is organized in a β-turn, probably of type II, that generates a bend in the centre of DB3. The two Tyr^{1}-Ile^{9} and Ala^{14}-Gly^{23} sequences are in extended or β-sheet conformation, and a salt bridge is present between the protonated amino group of Tyr^{1} and the carboxylate group of Gly^{23}. Point mutation studies, currently underway, have suggested the importance of hydrophobic interactions within the side chains of His^{8}, Phe^{15} and/or Tyr^{16} that, being closely located in the space due to the β-turn at positions 10–13, may generate an aromatic region that could be important for recognition at the receptor site. Syntheses of a cyclic analogue and a double constrained analogue of peptide DB3 are underway in order to obtain more precise information about conformation in solution and to value the reliability of the proposed theoretical model in the light of biological results.

Acknowledgements

This work was supported by grants from the Italian Ministry of Health, Progetto AIDS, Istituto Superiore di Sanita' and by the Italian National Council (CNR), Progetto FATMA.

REFERENCES

1. Q. J. Sattentau and R. A. Weiss (1988). The CD4 antigen: Physiological ligand and HIV receptor. *Cell 52*, 631–633.
2. L. A. Lasky, G. Nakamura, D. H. Smith, C. Fennie, C. Shimasaki, E. Patzer, P. Berman, T. Gregory and D. J. Capon (1987). Delineation of a region of the human immunodeficiency virus type 1 gp120 glycoprotein critical for interaction with the CD4 receptor. *Cell 50*, 975–985.
3. R. L. Willey, D. H. Smith, L. A. Lasky, T. S. Theodore, P. Earl, B. Moss, D. J. Capon and M. A. Martin (1988). *In vitro* mutagenesis identifies a site within the envelope gene of the human immunodeficiency virus that is critical for infectivity. *J. Virol. 62*, 139–147.

4. E. A. Berger, T. R. Fuerst and B. Moss (1988). A soluble recombinant polypeptide comprising the amino-terminal half of the extracellular region of the CD4 molecule contains an active binding site for human immunodeficiency virus. *Proc. Natl Acad. Sci. USA 85*, 2357–2361.
5. J. R. Rusche, K. Javaherian, C. McDanal, C. Petro, D. L. Lynn, R. Grimaila, A. Langlois, R. C. Gallo, L. O. Arthur, P. J. Fischinger, D. P. Bolognesi, S. D. Putney and T. J. Matthews (1988). Antibodies that inhibit fusion of human immunodeficiency virus-infected cells bind a 24-aminoacid sequence of the viral envelope, gp120. *Proc. Natl Acad. Sci. USA 85*, 3198–3202.
6. A. Condonnier, L. Montagnier and M. Emerman (1989). Single amino acid changes in HIV envelope affect viral tropism and receptor binding. *Nature 340*, 571–574.
7. L. K. Clayton, M. Sieh, D. A. Pious and E. L. Reinherz (1989). Identification of human CD4 residues affecting class II MHC versus HIV-1 gp120 binding. *Nature 339*, 548–551.
8. J. Arthos, K. C. Deen, M. A. Chairkin, J. A. Fornwald, G. Sathe, Q. J. Sattentau, P. R. Clapham, R. A. Weiss, J. S. McDougal, C. Pietropaolo, R. Axel, A. Truneh, P. J. Maddon and R. W. Sweet (1989). Identification of the residues in human CD4 critical for the binding of HIV. *Cell 57*, 469–481.
9. T. Mizukami, T. R. Fuerst, E. A. Berger and B. Moss (1988). Binding region for human immunodeficiency virus (HIV) and epitopes for HIV-blocking monoclonal antibodies of the CD4 molecules defined by site-directed mutagenesis. *Proc. Natl Acad. Sci. USA 85*, 9273–9277.
10. M. H. Brodsky, M. Warton, M. R. Myers and D. R. Littman (1990). Analysis of the site of CD4 that binds to the HIV envelope glycoprotein. *J. Immunol. 144*, 3078–3086.
11. D. Dowbenco, G. Nakamura, C. Fennie, C. Shimasaki, L. Riddle, R. Harris, T. Gregory and L. Lasky (1988). Epitope mapping of the human immunodeficiency virus type 1 gp120 with monoclonal antibodies. *J. Virol. 62*, 4703–4711.
12. C. B. Pert, J. M. Hill, M. R. Ruff, R. M. Berman, W. G. Robey, L. O. Arthur, F. W. Ruscetti and W. L. Farrar (1986). Octapeptide derived from the neuropeptide receptor-like pattern of antigen T4 in brain potently inhibits human immunodeficiency virus receptor binding and T-cell infectivity. *Proc. Natl Acad. Sci. USA 83*, 9254–9258.
13. K. Javaherian, A. J. Langlois, C. McDanal, K. L. Ross, L. I. Eckler, C. L. Jellis, A. T. Profy, J. R. Rusche, D. P. Bolognesi, S. D. Putney and T. J. Mattheus (1989). Principal neutralizing domain of the human immunodeficiency virus type I envelope protein. *Proc. Natl Acad. Sci. USA 86*, 6768–6772.
14. D. J. Capon, S. M. Chamow, J. Mordenti, S. A. Marsters, T. Gregory, H. Mitsuya, R. A. Byrn, C. Lucas, F. M. Wurm, J. E. Groopman, S. Broder and D. H. Smith (1989). Designing CD4 immunoadhesins for AIDS therapy. *Nature 337*, 525–531.
15. K. C. Deen, J. S. McDougal, R. Inacker, G. Folena-Wasserman, J. Rosenberg, P. J. Maddon, R. Alex and R. Sweet (1988). A soluble form of CD4 (T4) protein inhibits AIDS virus infection. *Nature 331*, 82–84.
16. R. A. Fisher, J. M. Bertonis, W. Meier, W. A. Johnson, D. S. Costopoulos, T. Liu, R. Tizard, B. D. Walker, M. S. Hirsch, R. T. Schooley and L. A. Flavell (1988). HIV infection is blocked *in vitro* by recombinant soluble CD4. *Nature 331*, 76–78.
17. R. E. Hussey, N. E. Richardson, M. Kowalski, N. R. Brown, H. Chang, R. F. Siciliano, T. Dorfman, B. Walker, J. Sodroski and E. L. Reinherz (1988). A soluble CD4 protein selectively inhibits HIV replication and syncytium formation. *Nature 331*, 78–81.
18. A. Taunecker, W. Luke and K. Karjalainen (1988). Soluble CD4 molecules neutralize human immunodeficiency virus type 1. *Nature 331*, 84–86.
19. P. L. Nara, K. M. Hwang, D. M. Rausch, J. D. Lifson and L. E. Eiden (1989). CD4 antigen-based antireceptor peptides inhibit infectivity of human immunodeficiency virus *in vitro* at multiple stages of the life cycle. *Proc. Natl. Acad. Sci. USA 86*, 7139–7143.
20. A. De Rossi, M. Pasti, F. Mammano, M. Panozzo, M. Dettin, C. Di Bello and L. Chieco-Bianchi (1991). Synthetic peptides from the principal neutralizing domain of human immunodeficiency virus type I (HIV-1) enhance HIV-1 infection through a CD4-dependent mechanism. *Virology 184*, 187–196.
21. M. Autiero, P. Abrescia, M. Dettin, C. Di Bello and J. Guardiola (1991). Binding to CD4 of synthetic peptides patterned on the principal neutralizing domain of the HIV-1 envelope glycoprotein. *Virology 185*, 820–828.
22. U. Piantini, O. W. Sørensen and R. R. Ernst (1982). Multiple quantum filters for elucidating NMR coupling networks. *J. Am. Chem. Soc. 104*, 6800–6801.
23. A. Bax and D. G. Davis (1985). MLEV-17-based two-dimensional homonuclear magnetization transfer spectroscopy. *J. Magn. Res. 65*, 355–360.
24. D. Neuhaus and M. Williamson: *The Nuclear Overhauser Effect*, VCH Publ., New York 1989.
25. H. Gausepohl, M. Kraft and R. W. Frank (1989). Asparagine coupling in Fmoc solid phase peptide synthesis. *Int. J. Peptide Protein Res. 34*, 287–294.
26. A. Perczel, G. Tusnady, M. Hallosi and G. D. Fasman (1991). Convex constraint analysis: a natural deconvolution of circular dichroism curves of proteins. *Protein Eng. 4*, 669–679.
27. K. Chandrasekhar, A. T. Profy and H. J. Dyson (1991). Solution conformational preferences of immunogenic peptides derived from the principal neutralizing determinant of the HIV-1 envelope glycoprotein gp120. *Biochemistry 30*, 9187–9194.
28. A. Zvi, R. Hiller and J. Anglister (1992). Solution conformation of peptide corresponding to the principal neutralizing determinant of HIV-1_{IIIB}: a two-dimen-

sional NMR study. *Biochemistry 31*, 6972–6979.
29. N. A. Roberts, J. A. Martin, D. Kinchington, A. V. Broadhurst, J. C. Craig, I. B. Duncan, S. A. Galpin, B. K. Handa, J. Kay and A. Krohn (1990). Rational design of peptide-based HIV proteinase inhibitor. *Science 248*, 358–361.
30. J. V. N. Vara Prasad, K. Houseman, R. Mueller and D. H. Rich in: *Peptides 1992*, C. H. Schneider and A. N. Eberle, Eds., p. 629–630, ESCOM, Leiden 1993.
31. A. De Rossi, M. Pasti, F. Mammano, M. Panozzo, M. Dettin, C. Di Bello and L. Chieco-Bianchi (1990). Peptidi sintetici atti a potenziare l'infettività del virus HIV-1. *National Patent* n°. 01244529.
32. A. Ranki, S. L. Valle and M. Krohn (1987). Long latency precedes overt seroconversion in sexually transmitted human immunodeficiency virus infection. *Lancet ii*, 589–593.
33. C. Di Bello, M. Dettin, L. Chieco-Bianchi, A. De Rossi, J. Guardiola and M. Autiero (1994). The use of synthetic peptides in the study of HIV-1/target cell interactions. *Curr. Topics Peptide Protein Res. 1*, 65–73.
34. G. J. La Rosa, J. P. Davide, K. Weihold, J. A. Waterbury, A. T. Profy, J. A. Lewis, A. J. Langlois, J. R. Dreesman, R. N. Boswell, P. Shadduck, L. H. Holley, M. Karplus, D. P. Bolognesi, t. J. Mattheus, E. A. Emini and S. D. Puney (1990). Conserved sequence and structural elements in the HIV-1 principal neutralizing determinant. *Science 249*, 932–935.